ISSN 2394-3777 (Print)
ISSN 2394-3785 (Online)
Available online at www.ijartet.com
International Journal of Advanced Research Trends in Engineering and Technology
Vol. 4, Special Issue 2, January 2017

An Inductively Active Filtering Method for Power-Quality Improvement of Distribution Networks with Nonlinear Loads

K.VENKATESH
M.Tech,
SREENIDHI INSTITUTE OF SCIENCE & TECHNOLOGY,
YAMNAMPET,
GHATKESKAR

K.V.V.P.CHARI
Associate Professor,
SREENIDHI INSTITUTE OF SCIENCE & TECHNOLOGY,
YAMNAMPET,
GHATKESKAR

Dr. P. RAVI BABU
Head of the Department EEE,
SREENIDHI INSTITUTE OF SCIENCE & TECHNOLOGY,
YAMNAMPET,
GHATKESKAR

***Abstract*: This paper proposes an inductively active filtering (IAF) method to comprehensively improve the power quality (PQ) for not only the distribution network (public grid) but also the power-supply system (nonlinear load) connected to the network. At first, a new main-circuit topology for implementing the IAF method is presented, which consists of an inductively filtered transformer and a fully tuned branch controlled by an inverter. It's operating principle and technical features are introduced by comparing with the traditional active filtering method. Based on this, the equivalent circuit is established and by means of mathematical modeling, the unique filtering mechanism of the IAF method is revealed in theory. Further, the control strategy of the FT branch and the impedance coordination for the inductively filtered transformer are designed based on theoretical analysis. A case study is investigated in detail to illustrate the operating characteristics of the IAF method. Both the theoretical and the case studies show that the IAF method can effectively prevent harmonic components from flowing into the primary (grid) winding of the transformer. Since the harmonic components are suppressed near the harmonic source, it is good for the power-supply system and especially good for the converter transformer. A Fuzzy Logic Controller (FLC) is used in the system to reduce the Total Harmonic Distortion (THD) in the grid currents.**

***Index Terms*: Active filtering method, converter transformer, distribution network, harmonic, inductive filtering method, power quality (PQ).**

NOMENCLATURE

APF	Active power filtering.
CSC	Current source converter.
DC	Direct current.
FT	Fully tuned.
HAPF	Hybrid active power filtering.
HPF	High-pass filter.
IAF	Inductively active filtering.
KCL	Kirchhoff's current law.
KVL	Kirchhoff's voltage law.
MV/LV	Medium voltage/low voltage.
PCC	Point of common coupling.
PI	Proportional integral.
PPF	Passive power filtering.
PWM	Pulse-width modulation.
VSC	Voltage-source converter.
VSI	Voltage-source inverter.
i_S	Source current.
i_P	Current at the primary side of a power transformer.
i_F	Output current of the APF or the FT branch.
i_L	Current at the nonlinear load side.
k_{12}, k_{32}	Turn ratio between the grid and the extended winding, between the delta and the extended winding, respectively.
V_{Aah},V_{Bbh},V_{Cch}	Three-phase voltage of the secondary extended winding.
V_{abh},V_{bch},V_{cah}	Three-phase voltage of the secondary delta winding.
V_{Agh},V_{Bgh},V_{Cgh}	Three-phase voltage of the primary winding.
V_{a0h},V_{b0h},V_{c0h}	Three-phase voltage on the FT branch.
I_{Aah},I_{Bbh},I_{Cch}	Three-phase current of the secondary extended winding.
I_{abh},I_{bch},I_{cah}	Three-phase current of the secondary delta winding.
I_{Agh},I_{Bgh},I_{Cgh}	Three-phase current of the primary winding.
I_{a0h},I_{b0h},I_{c0h}	Three-phase current on the FT branch.
Z_{h21},Z_{h23}	Short-circuit impedance between the extended and the grid winding,

ISSN 2394-3777 (Print)
ISSN 2394-3785 (Online)
Available online at www.ijartet.com
International Journal of Advanced Research Trends in Engineering and Technology
Vol. 4, Special Issue 2, January 2017

between the extended and the delta winding, respectively.

Z_{1h},Z_{2h},Z_{3h} Equivalent impedance of the primary, the secondary extended, and the secondary delta winding, respectively.

Z_{Fah},Z_{Fbh},Z_{Fch} Three-phase equivalent impedance of the FT branch.

I. INTRODUCTION

IN RECENT years, more power electronics are being applied in distribution networks. For example, wind power and solar energy are integrated into the network by means of current source converters (CSCs) and/or voltage-source converters (VSCs) [1]–[5]. The network also often provides power supply to various types of nonlinear loads, such as three-phase diode/ thyristor rectifiers for medium-voltage (MV) motor drives or large power industrial electrolysis [7]. Since the action of power electronics is inherently nonlinear, it inevitably brings power-quality (PQ) problems to the distribution network and to the power-supply system connected to the network [8], [9].

Power filtering is an effective way to solve the PQ problems. Currently, it includes PPF, APF, and HAPF methods [10]–[12]. However, these methods are mainly used to implement the filtering and the reactive power compensation at the PCC; thus, they are effective in solving the PQ problems of the public network, but cannot provide an effective solution for the power-supply system connected with the network. For example, a converter transformer is generally used in the rectifier/inverter system. Since there is no effective scheme on PQ improvement active on the power-electronics side of the transformer, all of the harmonic and the reactive power components flow freely in the windings of the transformer, which inevitably leads to a series of problems for the transformer, such as additional losses, temperature increase, vibration, and noise [13]–[16].

To overcome these problems, an inductive power filtering method was proposed in recent years [7], [17]–[21]. This method can prevent harmonic and reactive power components from flowing into the primary (grid) winding of the transformer, so it can effectively solve PQ problems of the power-supply system. In principle, this method uses the balance of a transformer's harmonic magnetic potential to carry out the power filtering. To get good filtering performance, it needs a necessary precondition. That is to say, to consider filtering the –order harmonic current, the FT branch connected to the winding tap should reach a series resonance at -order harmonic frequency. Up to now, the reactor-capacitor circuit is used to create such a precondition. However, in practice, due to the initial design error, material aging, and other influential factors, the FT branch cannot reach resonance completely. Besides, the current inductive filtering method can only suppress the fixed order harmonics by the fixed impedance design for the transformer and the FT branch. That is to say, the current inductive filtering system is designed based on the harmonic characteristics of the nonlinear load. If the load has varied harmonic generation or an unknown change of the harmonic characteristic, the filtering performance cannot be fully guaranteed.

Unlike the aforementioned filtering methods, this paper proposes an IAF method. It combines the advantages of inductive power filtering and active power filtering methods and can improve the PQ of the distribution network and the power-supply system itself. More important, it can track online the change in harmonic generation of the nonlinear load and always maintain effective filtering performance.

The structure of this paper is organized as follows. Section II presents the main circuit topology of the IAF method and describes the operating principle and technical features by comparison with the traditional APF method. Section III reveals the unique filtering mechanism in theory by detailed mathematical modeling. The controller structure, control strategy, and impedance coordination for the IAF method are designed in Section IV. A case study is performed in Section V to illustrate the filtering performance and operating characteristics of the IAF method. The conclusion is addressed in Section VI.

II. MAIN CIRCUIT TOPOLOGY

Fig. 1 compares the topologies of the traditional APF and the proposed IAF. As shown in Fig. 1(a), the traditional APF is generally configured

ISSN 2394-3777 (Print)
ISSN 2394-3785 (Online)
Available online at www.ijartet.com
International Journal of Advanced Research Trends in Engineering and Technology
Vol. 4, Special Issue 2, January 2017

at the PCC, and it usually adopts a coupling transformer to interface with the power system. For nonlinear loads, such as a large power industrial dc load, it needs the converter transformer to isolate the dc supply system from the distribution network. A power transformer with MV/LV windings is generally used to connect the nonlinear load with the MV distribution network.

For this generally used wiring scheme, when analyzing the harmonic flow, it can be found that the load current flows into the PCC through the converter transformer and the power transformer. These transformers have to suffer all of the harmonic and reactive power components from, which lead to additional losses, temperature increase, vibration, and noise for these two transformers. In practice, these transformers are generally located in different areas and the harmonics flows in the entire power-supply system, which may destroy the electro-magnetic environment of the system and surrounding areas. Furthermore, Fig. 1(b) shows another configuration where APF is located at the secondary side of the power transformer, that is, the primary side of the converter transformer. Although this configuration can effectively solve the PQ problems of the power transformer, the converter transformer still has to face all of the PQ problems caused by the nonlinear load. Here, it should be noted that the commutation process of CSC needs the support of commutation reactance provided by the converter transformer. When APF is directly parallel with the converter bridge, the commutation process may be affected by the impedance of the APF. Thus, in a traditional scheme, the PQ problems cannot be avoided for the converter transformer.

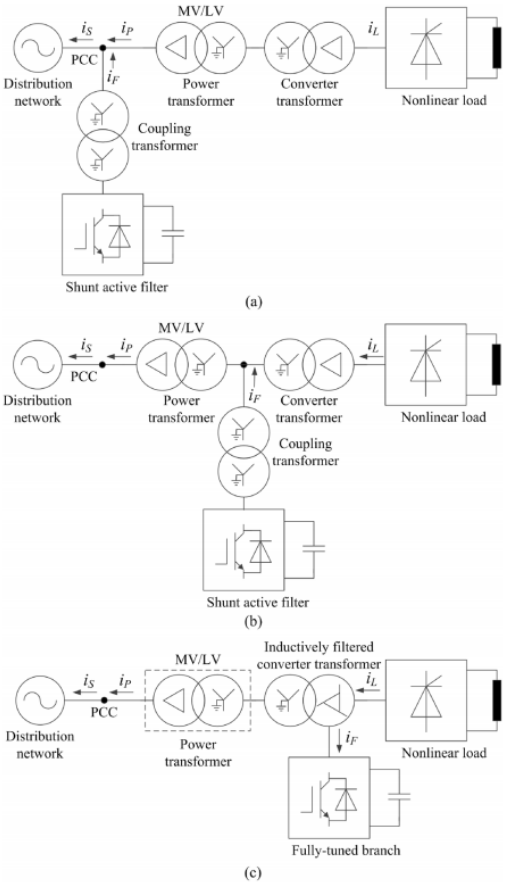

Fig. 1: Comparison of topologies: (a) traditional APF located at the PCC side, (b) traditional APF located at the primary side of the converter transformer, and (c) proposed IAF coordinated with the converter transformer.

Unlike the traditional APF configurations, Fig. 1(c) shows the topology of the proposed IAF. In this figure, there is an inductively filtered converter transformer between the nonlinear load and the power transformer. This converter transformer has a special wiring scheme. Its secondary winding adopts extended delta wiring. Between the extended windings and the delta windings, there is a linking point connected to the FT branch. Details of the transformer and FT branch will be mentioned later. The FT branch is controlled by an inverter, and it can attract almost all of the harmonic components flowing into this branch. Under these conditions, the harmonic magnetic potential is balanced between the extended windings and the delta windings; thus, there are very few harmonic components in the

ISSN 2394-3777 (Print)
ISSN 2394-3785 (Online)
Available online at www.ijartet.com
International Journal of Advanced Research Trends in Engineering and Technology
Vol. 4, Special Issue 2, January 2017

primary winding of the converter transformer. In this way, the harmonic components are suppressed near the nonlinear load (harmonic source). It means the path of harmonic flow is limited in a small area, which significantly reduces the impact of harmonics on the supply system. [6] presented a short overview on widely used microwave and RF applications and the denomination of frequency bands. The chapter start outs with an illustrative case on wave propagation which will introduce fundamental aspects of high frequency technology.

Moreover, since the current in the primary winding represents a good sinusoid, we may even integrate the MV winding of the power transformer with the primary winding, and there is no need to configure an independent power transformer to connect the distribution network.

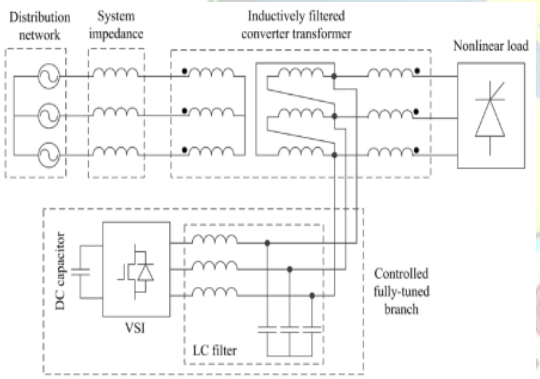

Fig. 2. Wiring scheme of IAF.

III. MATHEMATICAL MODELING AND ANALYSIS OF THE FILTERING MECHANISM

The physical implication of the IAF method can be simply described as follows: the FT branch detects the harmonic components of the load-side current, predicts the harmonic components that flow into the branch, and shapes an opposite harmonic components to eliminate them; at the same time, once the harmonic components flow into the secondary extended winding, the secondary delta winding inducts corresponding components to balance them, then there is none of these components in the primary winding.

In the following subsections, the filtering mechanism and control principle will be explained by establishing the equivalent circuit model and the mathematical model.

A. Equivalent Circuit Model

Fig. 2 shows the wiring scheme of the IAF. In this scheme, the secondary winding of the converter transformer adopts extended-delta wiring. For each phase, there is a linkage point, which is connected with the controlled FT branch, between the extended and the delta windings. This special wiring on the secondary winding aims at balancing harmonic magnetic potential surrounding secondary winding; thus, harmonic currents cannot be inducted into the primary (grid) winding. The details will be discussed in Section III-C The branch consists of the filter, VSI, and dc capacitor. The control strategy and structure will be proposed in Section IV.

According to Fig. 2, the three-phase equivalent circuit model for the inductively filtered converter transformer and the FT branch can be established, as shown in Fig. 3. In this model, each winding of the transformer is equivalent to impedance and the FT branch can be seen as controlled impedance. For conveniently analyzing the filtering mechanism, the flow directions of the fundamental and harmonic currents from the load to the grid side are defined by solid arrows.

B. Basic Mathematical Model

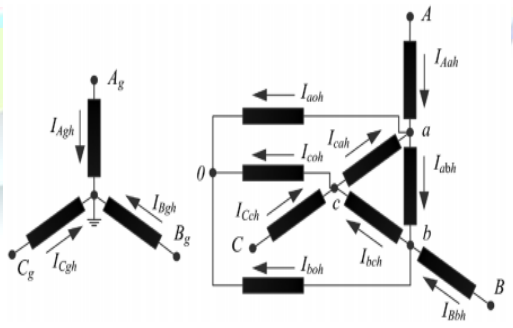

Fig. 3. Three-phase equivalent circuit.

According to the theory of multi winding transformers and combining the equivalent circuit model shown in Fig. 3, the voltage equations at the fundamental and the harmonic frequencies can be obtained as follows:

ISSN 2394-3777 (Print)
ISSN 2394-3785 (Online)
Available online at www.ijartet.com
International Journal of Advanced Research Trends in Engineering and Technology
Vol. 4, Special Issue 2, January 2017

$$\begin{cases} V_{Aah} - k_{12}^{-1}V_{Agh} = -k_{12}I_{Agh}Z_{h21} - k_{32}I_{abh} \\ V_{Aah} - k_{32}^{-1}V_{abh} = -k_{32}I_{abh}Z_{h23} - k_{12}I_{Agh} \\ V_{Bbh} - k_{12}^{-1}V_{Bgh} = -k_{12}I_{Bgh}Z_{h21} - k_{32}I_{bch} \\ V_{Bbh} - k_{32}^{-1}V_{bch} = -k_{32}I_{bch}Z_{h23} - k_{12}I_{Bgh} \\ V_{Cch} - k_{12}^{-1}V_{Cgh} = -k_{12}I_{Cgh}Z_{h21} - k_{32}I_{cah} \\ V_{Cch} - k_{32}^{-1}V_{cah} = -k_{32}I_{cah}Z_{h23} - k_{12}I_{Cgh} \end{cases}$$

Where Z_{h21} and Z_{h23} can be obtained by the short-circuit test, and Z_{2h} is calculated based on Z_{h21}, Z_{h23}, and Z_{h13} (here the superscript ' means the impedance value is reduced into the side of the secondary extended winding), that is to say

$$Z_{2h} = \frac{1}{2}\left(Z_{h21} + Z_{h23} - Z'_{h13}\right). \tag{2}$$

According to the principle of transformer magnetic potential balance and ignoring very few exciting currents, the current equations at the fundamental and the harmonic frequencies can be obtained as follows:

$$\begin{cases} I_{Aah} + k_{12}I_{Agh} + k_{32}I_{abh} = 0 \\ I_{Bbh} + k_{12}I_{Bgh} + k_{32}I_{bch} = 0 \\ I_{Cch} + k_{12}I_{Cgh} + k_{32}I_{cah} = 0. \end{cases} \tag{3}$$

According to Kirchhoff's current law (KCL), the following equations can be obtained to illustrate the relationship between the load-side current and the winding current, between the winding current and the FT branch current, respectively, that is

$$\begin{cases} I_{Aah} = I_{ALh} \\ I_{Aah} = I_{abh} + I_{a0h} - I_{cah} \\ I_{Bbh} = I_{BLh} \\ I_{Bbh} = I_{bch} + I_{b0h} - I_{abh} \\ I_{Cch} = I_{CLh} \\ I_{Cch} = I_{cah} + I_{c0h} - I_{bch} \\ I_{abh} + I_{bch} + I_{cah} = 0 \\ I_{Aah} + I_{Bbh} + I_{Cch} = 0 \end{cases} \tag{4}$$

where I_{ALh}, I_{BLh}, and I_{CLh} can be used to express the harmonic characteristics of the nonlinear load.

Furthermore, according to Kirchhoff's voltage law (KVL), the equations which express the relationship between trans former windings' and FT branch voltage, can be obtained as follows:

$$\begin{cases} V_{abh} = -V_{b0h} + V_{a0h} \\ V_{bch} = -V_{c0h} + V_{b0h} \\ V_{cah} = -V_{a0h} + V_{c0h} \\ V_{a0h} = I_{a0h}Z_{Fah} \\ V_{b0h} = I_{b0h}Z_{Fbh} \\ V_{c0h} = I_{c0h}Z_{Fch} \end{cases} \tag{5}$$

where Z_{Fah}, Z_{Fbh}, and Z_{Fch} are controlled by the VSI.

Equations (1)–(5) construct the mathematical model for the inductively filtered transformer and the FT branch. Based on this model, it is easy to investigate the operating characteristics and the special filtering characteristics that the IAF method has. It also provides a guideline for the impedance coordination and the controller design of the IAF system.

C. Filtering Characteristics

According to (1)–(5), the current, from the load side to the primary winding side of the transformer, can be deduced as follows:

$$\begin{cases} I_{Agh} = -\frac{k_{12}(Z_{3h}+3Z_{Fh})+k_{12}k_{32}Z_{Fh}}{k_{12}^2(Z_{3h}+3Z_{Fh})+k_{32}^2Z_{1h}}I_{ALh} \\ \quad + \frac{k_{12}k_{32}Z_{Fh}}{k_{12}^2(Z_{3h}+3Z_{Fh})+k_{32}^2Z_{1h}}I_{BLh} \\ I_{Bgh} = -\frac{k_{12}(Z_{3h}+3Z_{Fh})+k_{12}k_{32}Z_{Fh}}{k_{12}^2(Z_{3h}+3Z_{Fh})+k_{32}^2Z_{1h}}I_{BLh} \\ \quad + \frac{k_{12}k_{32}Z_{Fh}}{k_{12}^2(Z_{3h}+3Z_{Fh})+k_{32}^2Z_{1h}}I_{CLh} \\ I_{Cgh} = -\frac{k_{12}(Z_{3h}+3Z_{Fh})+k_{12}k_{32}Z_{Fh}}{k_{12}^2(Z_{3h}+3Z_{Fh})+k_{32}^2Z_{1h}}I_{CLh} \\ \quad + \frac{k_{12}k_{32}Z_{Fh}}{k_{12}^2(Z_{3h}+3Z_{Fh})+k_{32}^2Z_{1h}}I_{ALh}. \end{cases} \tag{6}$$

Similarly, current from the load side to the secondary delta winding side can be obtained as follows:

$$\begin{cases} I_{abh} = -\frac{k_{32}Z_{1h}-k_{12}^2Z_{Fh}}{k_{12}^2(Z_{3h}+3Z_{Fh})+k_{32}^2Z_{1h}}I_{ALh} \\ \quad - \frac{k_{12}^2Z_{Fh}}{k_{12}^2(Z_{3h}+Z_{Fh})+k_{32}^2Z_{1h}}I_{BLh} \\ I_{bch} = -\frac{k_{32}Z_{1h}-k_{12}^2Z_{Fh}}{k_{12}^2(Z_{3h}+3Z_{Fh})+k_{32}^2Z_{1h}}I_{BLh} \\ \quad - \frac{k_{12}^2Z_{Fh}}{k_{12}^2(Z_{3h}+Z_{Fh})+k_{32}^2Z_{1h}}I_{CLh} \\ I_{cah} = -\frac{k_{32}Z_{1h}-k_{12}^2Z_{Fh}}{k_{12}^2(Z_{3h}+3Z_{Fh})+k_{32}^2Z_{1h}}I_{CLh} \\ \quad - \frac{k_{12}^2Z_{Fh}}{k_{12}^2(Z_{3h}+Z_{Fh})+k_{32}^2Z_{1h}}I_{ALh}. \end{cases} \tag{7}$$

According to (6), it can be found that the filtering performance of the IAF method highly depends on the equivalent impedance of the secondary delta winding and the FT branch (Z_{3h} and Z_{Fh}). Ideally, to ensure that the h-order harmonic current does not flow into the grid winding, that is to say,

ISSN 2394-3777 (Print)
ISSN 2394-3785 (Online)
Available online at www.ijartet.com
International Journal of Advanced Research Trends in Engineering and Technology
Vol. 4, Special Issue 2, January 2017

$I_{Agh} = I_{Bgh} = I_{Cgh} = 0$, the impedance parameters at the h–order harmonic frequency should satisfy the following constraint:

$$Z_{3h} = Z_{Fh} = 0. \quad (8)$$

Actually, (8) gives a perfect example of harmonic suppression. In practice, we only need to guarantee that at the fundamental frequency, the equivalent reactance of the secondary winding and the FT branch are approximately equal to 0, that is, $L_3 \approx 0$ and $L_F \approx 0$, or these two reactance are much less than the equivalent reactance of the grid winding, that is, $L_3 \ll L_1$ and $L_F \ll L_1$, then the effective filtering performance can be reached.

Further, when considering the implementation of the IAF method, according to (4), (7) and (8), the equations about the magnetic potential balance at the h-order harmonic frequency can be obtained as follows:

$$\begin{cases} I_{abh} = -k_{32}^{-1} I_{Aah} \\ I_{bch} = -k_{32}^{-1q} I_{Bbh} \\ I_{cah} = -k_{32}^{-1} I_{Cch}. \end{cases} \quad (9)$$

Equation (9) indicates that the harmonic magnetic potential of the inductively filtered converter transformer is balanced between the secondary extended and delta winding, and the primary (grid) winding does not participate in such harmonic magnetic potential balance. In other words, harmonic currents cannot flow into the grid winding, and they are isolated away from the grid winding and the grid side.

IV. CONTROLLER DESIGN

For the control strategy of the IAF method, a very important task is how to attract all of the harmonic components flowing from the load side into the FT branch and create the precondition for the harmonic magnetic potential balance between the secondary extended and delta winding. Here, the active technique is used for this task. Unlike the existing APF method, in the IAF method, the control object of the FT branch includes the following parts: 1) track the change of harmonic components at the load side; 2) predict the amount of harmonic components that should flow into the FT branch; and 3) generate the opposite harmonic components to eliminate them. In this way, the FT branch represents a resonant state at the harmonic frequencies, that is, $Z_{Fh}=0$, which is the precondition for the implementation of the IAF method, as shown in (8).

In the following subsections, the basic control flow will be presented and then the essential part, which is about how to calculate the amount of the harmonic current attracted to the FT branch, will be investigated in detail.

A. Control Flow

The control diagram for the FT branch is presented as shown in Fig. 4. In general, the control flow of the FT branch includes the following parts:

1) Calculation of and : Based on the detected three-phase voltage (V_{AL}, V_{BL}, and V_{CL}) and current (I_{AL}, I_{BL}, and I_{CL}) at the load side, the instantaneous real and reactive power based on α and β quantities are obtained by using the p–q theory [22]. Generally, the phase voltage at the ac valve side of the converter bridge represents nonsinusoidal; thus, it is difficult to accurately transform the three-phase voltage into α and β quantities. To overcome this problem, we can measure the voltage at the primary (grid) side of the converter transformer and indirectly obtain the voltage at the load side by using the potential transformer (PT) with the same wiring to the converter transformer, or consider the phase-shift factor of the converter transformer and indirectly calculate the valve-side voltage by using the grid-side voltage.

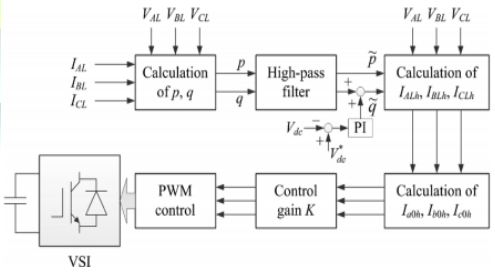

Fig. 4. Control diagram for the fully tuned branch.

2) High-Pass Filter (HPF): The HPF is used to filter the dc and the low-frequency components in p and q ; thus, the high-frequency components remain, that is, p and q. The performance of the HPF highly depends on proper setting of the characteristic frequency f_c. Here, in order to attract the full

ISSN 2394-3777 (Print)
ISSN 2394-3785 (Online)
Available online at www.ijartet.com
International Journal of Advanced Research Trends in Engineering and Technology
Vol. 4, Special Issue 2, January 2017

harmonic components from the load-side current to the FT branch and, at the same time, prevent the fundamental component, f_c is set as 100 Hz.

3) Calculation of Harmonic Components of the Load-Side Current: The harmonic components of the load-side current are extracted by p, q, and the load-side voltage (V_{AL}, V_{BL}, and V_{CL}). Besides, the dc voltage of the VSI is controlled by a proportional-integral (PI) controller. The output of the PI controller is an additional component to the filtered reactive power at the q-axis.

4) Calculation of Harmonic Components Attracted to the FT Branch: Due to the constraints among the harmonic currents in the secondary extended and delta winding, the harmonic components attracted to the FT branch, that is, the I_{a0h}, I_{b0h}, and I_{c0h} shown in Fig. 4 are not from the load side directly. They should be calculated based on the basic mathematical model in Section V-B and the analysis of filtering characteristics in Section V-C. The detailed calculation will be proposed in the next subsection.

5) Control Gain K: The calculated currents I_{a0h}, I_{b0h}, and I_{c0h} are multiplied by to generate the current reference for the pulse-width modulation (PWM) of the VSI. The reference is compared with the output of the ac current of the VSI, which is used to produce the PWM waves for the independent current control of the VSI.

B. Calculation of Harmonic Current Attracted to the FT Branch

As mentioned before, the harmonic currents I_{a0h}, I_{b0h}, and I_{c0h} attracted from the load side to the FT branch, are determined by the harmonic currents in the secondary windings of the converter transformer. According to (4) and (7), they can be obtained conveniently, as shown in (10).

$$\begin{cases} I_{a0h}=\left[1+\dfrac{k_{32}Z_{1h}-2k_{12}^2Z_{Fh}}{k_{12}^2(Z_{3h}+3Z_{Fh})+k_{32}^2Z_{1h}}\right]I_{ALh}+\dfrac{k_{12}^2Z_{Fh}}{k_{12}^2(Z_{3h}+3Z_{Fh})+k_{32}^2Z_{1h}}I_{BLh}-\dfrac{k_{32}Z_{1h}-2k_{12}^2Z_{Fh}}{k_{12}^2(Z_{3h}+3Z_{Fh})+k_{32}^2Z_{1h}}I_{CLh} \\ I_{b0h}=\left[1+\dfrac{k_{32}Z_{1h}-2k_{12}^2Z_{Fh}}{k_{12}^2(Z_{3h}+3Z_{Fh})+k_{32}^2Z_{1h}}\right]I_{BLh}+\dfrac{k_{12}^2Z_{Fh}}{k_{12}^2(Z_{3h}+3Z_{Fh})+k_{32}^2Z_{1h}}I_{CLh}-\dfrac{k_{32}Z_{1h}-2k_{12}^2Z_{Fh}}{k_{12}^2(Z_{3h}+3Z_{Fh})+k_{32}^2Z_{1h}}I_{ALh} \\ I_{c0h}=\left[1+\dfrac{k_{32}Z_{1h}-2k_{12}^2Z_{Fh}}{k_{12}^2(Z_{3h}+3Z_{Fh})+k_{32}^2Z_{1h}}\right]I_{CLh}+\dfrac{k_{12}^2Z_{Fh}}{k_{12}^2(Z_{3h}+3Z_{Fh})+k_{32}^2Z_{1h}}I_{ALh}-\dfrac{k_{32}Z_{1h}-2k_{12}^2Z_{Fh}}{k_{12}^2(Z_{3h}+3Z_{Fh})+k_{32}^2Z_{1h}}I_{BLh}. \end{cases} \quad (10)$$

It can be seen from (10) that the attracted harmonic currents on the FT branch highly depend on the impedance parameters Z_{1h}, Z_{3h}, and Z_{Fh}. When considering the application of the IAF method, (8) is satisfied. Under this condition, (10) can be simplified as follows:

$$\begin{cases} I_{a0h}=\left(1+k_{32}^{-1}\right)I_{ALh}-k_{32}^{-1}I_{CLh} \\ I_{b0h}=\left(1+k_{32}^{-1}\right)I_{BLh}-k_{32}^{-1}I_{ALh} \\ I_{c0h}=\left(1+k_{32}^{-1}\right)I_{CLh}-k_{32}^{-1}I_{BLh}. \end{cases} \quad (11)$$

In fact, (11) expresses the total amount of harmonic currents that flow into the FT branch. Correspondingly, the FT branch should be controlled to generate the opposite harmonic currents to eliminate them, which means the mentioned in Section IV-A should be a negative value. In this way, the FT branch represents a "short-circuit" state at the harmonic frequencies. It can attract the harmonic currents expressed by (11) to the FT branch; thus, the harmonic magnetic potential balance is realized between the extended and the delta winding of the transformer.

Moreover, based on (11), the volt-ampere rating of the controlled FT branch can be obtained as follows:

$$P_{\mathrm{FT}}=\sqrt{3}\times\frac{V_{\mathrm{dc}}}{\sqrt{2}}\times\frac{I_F}{\sqrt{2}} \quad (12)$$

Where V_{dc} is the dc voltage of VSI; and I_F is the output current of the controlled FT branch, for an ideal balanced three-phase system $I_F=I_{a10h}=I_{b10h}=I_{c10h}$.

V. FUZZY LOGIC CONTROLLER

In FLC, basic control action is determined by a set of linguistic rules. These rules are determined by the system. Since the numerical variables are converted into linguistic variables, mathematical modeling of the system is not required in FC. The FLC comprises of three parts: fuzzification, interference engine and defuzzification.

The FC is characterized as i. seven fuzzy sets for each input and output. ii. Triangular membership functions for simplicity. iii. Fuzzification using continuous universe of discourse. iv. Implication using Mamdani's, 'min' operator. v. Defuzzification using the height method.

ISSN 2394-3777 (Print)
ISSN 2394-3785 (Online)
Available online at www.ijartet.com
International Journal of Advanced Research Trends in Engineering and Technology
Vol. 4, Special Issue 2, January 2017

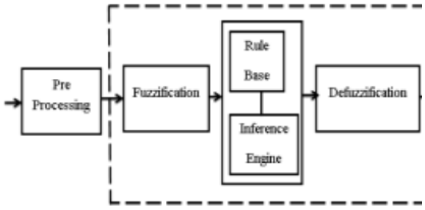

Fig. 5: Fuzzy logic controller

Fuzzification: Membership function values are assigned to the linguistic variables, using seven fuzzy subsets: NB (Negative Big), NM (Negative Medium), NS (Negative Small), ZE (Zero), PS (Positive Small), PM (Positive Medium), and PB (Positive Big). The partition of fuzzy subsets and the shape of membership CE(k) E(k) function adapt the shape up to appropriate system. The value of input error and change in error are normalized by an input scaling factor

Table I Fuzzy Rules

Change in error	Error						
	NB	NM	NS	Z	PS	PM	PB
NB	PB	PB	PB	PM	PM	PS	Z
NM	PB	PB	PM	PM	PS	Z	Z
NS	PB	PM	PS	PS	Z	NM	NB
Z	PB	PM	PS	Z	NS	NM	NB
PS	PM	PS	Z	NS	NM	NB	NB
PM	PS	Z	NS	NM	NM	NB	NB
PB	Z	NS	NM	NM	NB	NB	NB

In this system the input scaling factor has been designed such that input values are between -1 and +1. The triangular shape of the membership function of this arrangement presumes that for any particular E(k) input there is only one dominant fuzzy subset. The input error for the FLC is given as

$$E(k) = \frac{P_{ph(k)} - P_{ph(k-1)}}{V_{ph(k)} - V_{ph(k-1)}} \quad (13)$$

$$CE(k) = E(k) - E(k-1) \quad (14)$$

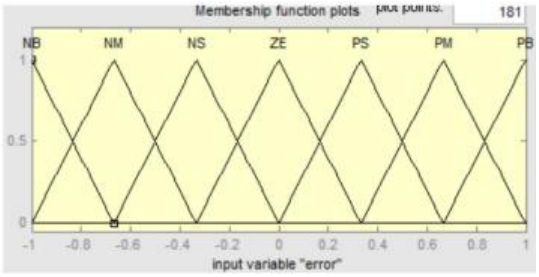

Fig. 6: Membership functions

Inference Method: Several composition methods such as Max–Min and Max-Dot have been proposed in the literature. In this paper Min method is used. The output membership function of each rule is given by the minimum operator and maximum operator. Table 1 shows rule base of the FLC.

Defuzzification: As a plant usually requires a non-fuzzy value of control, a defuzzification stage is needed. To compute the output of the FLC, „height" method is used and the FLC output modifies the control output. Further, the output of FLC controls the switch in the inverter. In UPQC, the active power, reactive power, terminal voltage of the line and capacitor voltage are required to be maintained. In order to control these parameters, they are sensed and compared with the reference values. To achieve this, the membership functions of FC are: error, change in error and output.

The set of FC rules are derived from

$$u=-[\alpha E + (1-\alpha)*C] \quad (15)$$

Where α is self-adjustable factor which can regulate the whole operation. E is the error of the system, C is the change in error and u is the control variable. A large value of error E indicates that given system is not in the balanced state. If the system is unbalanced, the controller should enlarge its control variables to balance the system as early as possible. set of FC rules is made using Fig. 6 is given in Table 1.

VI. SIMULATION RESULTS

In order to validate the theoretical results mentioned before and reveal the special operating characteristics of the IAF method, a detailed case study on the distribution network with the nonlinear

ISSN 2394-3777 (Print)
ISSN 2394-3785 (Online)
Available online at www.ijartet.com
International Journal of Advanced Research Trends in Engineering and Technology
Vol. 4, Special Issue 2, January 2017

load, as shown in Fig. 3, was carried out by using PSCAD/EMTDC [23]. Here, we are concerned with the power quality of the public grid and the connected power-supply system for the nonlinear load. The traditional APF method is also simulated to compare with the proposed IAF method.

Table II shows the comparison on the basic design parameters of the new and the traditional converter transformer. Table III shows the design parameters of the LC filter used by the traditional APF and the proposed IAF method, respectively. Both the traditional APF and the new IAF methods adopt the similar controller structure like Fig. 4. The difference is the calculation of the compensation current. For the new IAF method, it uses (11) to calculate the amount of the harmonic currents generated by VSI. According to design parameters shown in Table II, k^{-1}_{32} is equal to 0.5778.

TABLE II
BASIC DESIGN PARAMETERS OF THE NEW AND TRADITIONAL CONVERTER TRANSFORMER

	Rating /MVA	Wiring mode	Impedance /pu	Voltage /kV
New converter transformer	0.02	Wye /Extended-delta	$Z_{12} = 0.20$ $Z_{13} = 0.02$ $Z_{23} = 0.18$	$V_1 = 0.1155$ $V_2 = 0.0598$ $V_3 = 0.1035$
Traditional converter transformer	0.02	Wye/Delta	$Z_{12} = 0.20$	$V_1 = 0.1155$ $V_2 = 0.2000$

TABLE III
DESIGN PARAMETERS OF THE LC FILTER

	L/mH	$C/\mu F$
IAF method	0.6	0.02
APF method	1.0	0.1

Based on Table II and (12), the rating of the controlled FT branch can be compared to that of the traditional APF. More specifically, in this case study, the VSI, adopted by APF and IAF methods, has the same value dc voltage reference . For the IAF method, $I_F=I_{a10h}=(1+ k^{-1}_{32}-k^{-1}_{32}e^{-j120})I_L$ while for the APF method, according to Table II, $I_F=(0.2/0.1155)I_L$. Here, I_L is the nonlinear load-side current. Therefore, the rating of the controlled FT branch is 1.1161 times that of the APF. However, it should be noted that the rating is varied with the turn ratios of the converter transformer.

This case study on the IAF method is performed from the following three aspects: 1) filtering performance with comparison to the APF method; 2) dynamic response when applying the IAF method in the distribution network; and 3) dynamic response to variation of the nonlinear load.

A. Test 1: Filtering Performance

Figs. 7 and 8 show the steady-state responses of the traditional APF and the proposed IAF methods, respectively. It can be seen from Figs. 7(a) and 8(a) that regardless of whether using the APF or the IAF method, the current at the load side has a similar harmonic characteristic, which is determined by the type of nonlinear load. It can also be seen from Figs. 7(c) and 8(c) that both filtering methods can effectively suppress the harmonic currents at the ac grid side, thus improving the power quality of the public distribution network.


(a)

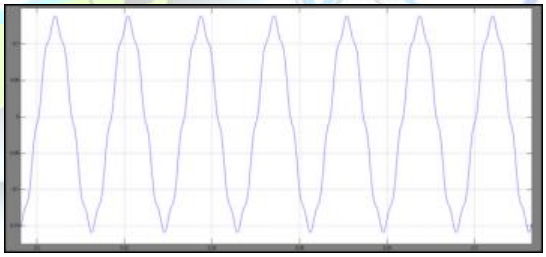
(b)

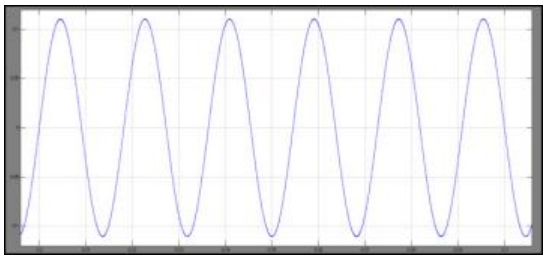
(c)

ISSN 2394-3777 (Print)
ISSN 2394-3785 (Online)
Available online at www.ijartet.com
International Journal of Advanced Research Trends in Engineering and Technology
Vol. 4, Special Issue 2, January 2017

Fig. 7: Steady-state response of the system with the traditional APF method. (a) Current at the load side. (b) Current in the grid winding of the transformer.
(c) Current at the ac grid side.

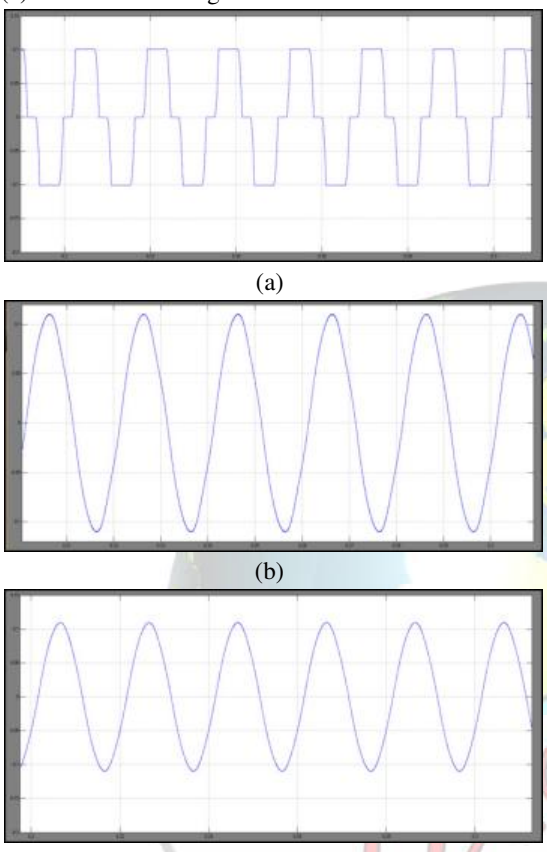

(a)

(b)

(c)

Fig. 8: Steady-state response of the system with the proposed IAF method. (a) Current at the load side. (b) Current in the grid winding of the transformer. (c) Current at the ac grid side.

However, by comparing Figs. 7(b) and 8(b), it is clear that the traditional APF method cannot carry out harmonic suppression in the grid winding; thus, there are heavy harmonic components. But the proposed IAF method can significantly reduce the harmonic content in the grid winding; thus, the waveform of the grid winding current is represented as a good sinusoidal.

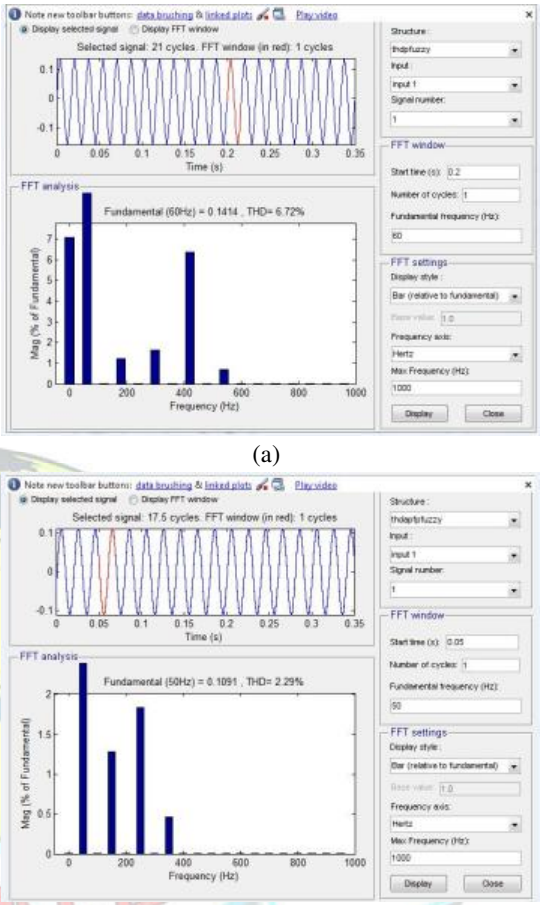

(a)

(b)

Fig. 7: FFT results on the current waveform in the grid winding when using (a) traditional APF method [see Fig. 7(b)] and using (b) proposed IAF method [see Fig. 8(b)].

It means the IAF method cannot only solve the power-quality problem to the public grid but also to the power-supply system connected with the nonlinear load. Furthermore, Fig. 9 gives more details about the main order harmonic currents in the grid winding, when implementing the traditional APF method or the proposed IAF method. From this figure, it can be seen that the APF method cannot suppress harmonic currents in the grid winding of the converter transformer. The total harmonic distortion (THD) is 20.26%. When using the IAF method, the harmonic currents in the grid winding are suppressed successfully. The THD is reduced to 4.18%.

B. Test 2: Dynamic Response When Switching on the FT Branch

ISSN 2394-3777 (Print)
ISSN 2394-3785 (Online)
Available online at www.ijartet.com
International Journal of Advanced Research Trends in Engineering and Technology
Vol. 4, Special Issue 2, January 2017

In order to assess the impact of the IAF method on the operation of the nonlinear load, the following case is considered:

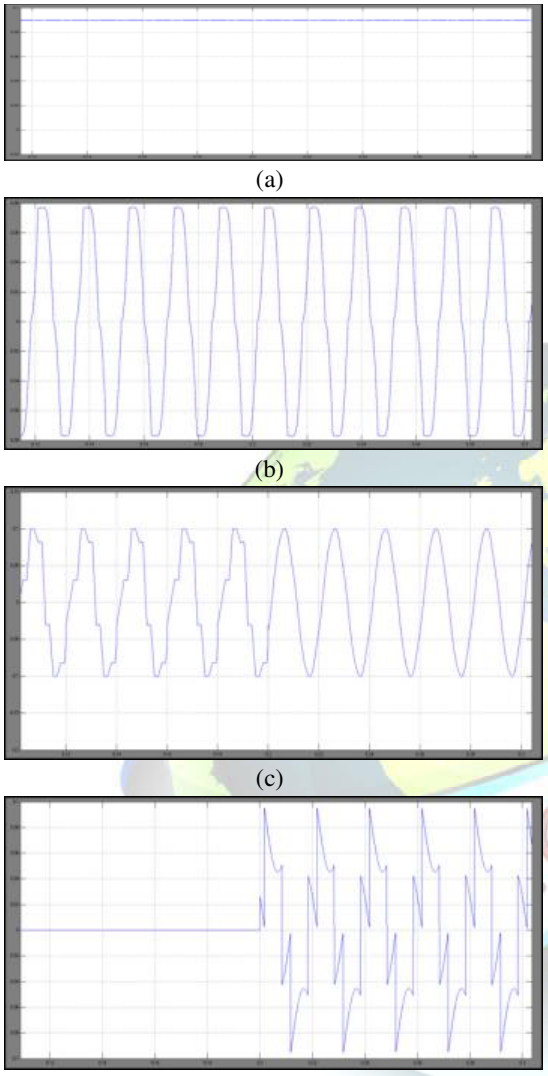

(a)

(b)

(c)

(d)

Fig. 10: Dynamic response when switching on the FT branch. (a) Current at the dc side of the nonlinear load. (b) Current at the ac valve side of the nonlinear load. (c) Current in the grid winding. (d) Current on the FT branch.

Before 0.2 s, the load and also the related power supply system operate without the IAF method and at 0.2 s, the FT branch is switched on to implement the IAF method. Fig. 10 shows the dynamic response of the test system. It can be seen From Fig. 10(a) and (b) that the switching of the FT branch has no influence on the operation of the load. Both currents at the dc side and the ac valve side are stable before and after the switching the FT branch, which means that the IAF method does not affect the operation of the load and the connected power supply system. On the other hand, from Fig. 10(b) and (c), it can be seen that when switching the FT branch, which means the implementation of the IAF method, the branch can attract the harmonic components from the load side; thus, the harmonic currents in the grid winding are reduced significantly. The results coincide with the theoretical analysis.

C. Test 3: Dynamic Response to Nonlinear Load Variation

In this subsection, the filtering performance under the variation of the nonlinear load is investigated to further assess the IAF method. At 0.3 s, the impedance of the load of the dc side (shown in Fig. 2) is reduced to express the load variation. Fig. 11 shows the dynamic response of the test system. It can be seen from Fig. 11(a) that with the change of the load, the dc supply current is increased from around 0.09 to 0.22 kA.

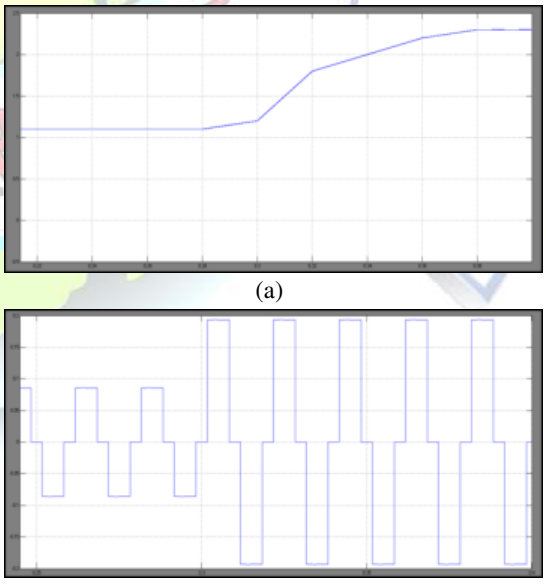

(a)

(b)

ISSN 2394-3777 (Print)
ISSN 2394-3785 (Online)
Available online at www.ijartet.com
International Journal of Advanced Research Trends in Engineering and Technology
Vol. 4, Special Issue 2, January 2017

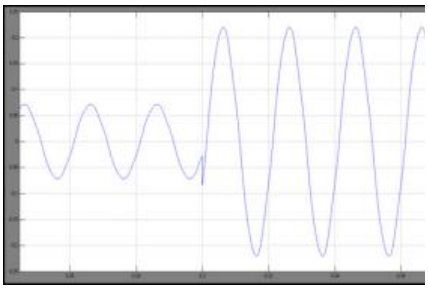

(c)

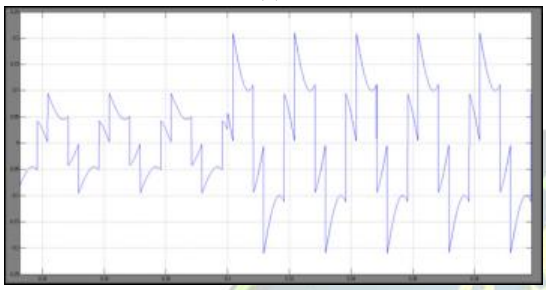

(d)

Fig. 11: Dynamic response to the variation of the nonlinear load. (a) Current at the dc side of the nonlinear load. (b) Current at the ac valve side of the nonlinear load. (c) Current in the grid winding. (d) Current on the FT branch.

The nonlinear load generates more harmonic components at the ac valve side, as shown in Fig. 11(b). However, the IAF can track the load variation successfully and the FT branch attracts more harmonic currents [see Fig. 11(d)]; thus, the current waveform in the grid winding of the converter transformer can always maintain a good sinusoid, as shown in Fig. 11(c).

VII. CONCLUSION

In this paper, an IAF method, which is characterized as an inductively filtered converter transformer and a controlled FT branch, is proposed to improve the PQ of the distribution network (public grid) and the power-supply system (power consumer side) connected with nonlinear loads. The three-phase equivalent circuit model and the basic mathematical model are established to express such a new power filtering method. Based on the extension of the mathematical model, the control method and controller structure for the FT branch are designed, which is used to create the precondition for the balance of the harmonic magnetic potential in the windings of the converter transformer.

The theoretical results indicate that by means of the IAF method, the harmonic currents are balanced out in the secondary winding of the converter transformer; thus, there are not any or only a few harmonic currents inducted into the primary (grid) winding. The case results coincide with the theoretical analysis and illustrate the good filtering performance under a dynamic state (e.g., variation of the nonlinear load and the switching of the FT branch). The IAF method can contribute PQ improvement for the public network and the power consumer. It may also reduce the need for power transformers that isolate the nonlinear loads from the distribution network. It has potential application in industrial power-supply systems and distribution networks interfaced with distributed generation.

REFERENCES

[1] Z. Chen, F. Blaabjerg, and J. K. Pedersen, "Hybrid compensation arrangement in dispersed generation systems," *IEEE Trans. Power Del.*, vol. 20, no. 2, pt. 2, pp. 1719–1727, Apr. 2005.

[2] R. Li, S. Bozhko, and G. Asher, "Frequency control design for offshore wind farm grid with LCC-HVDC link connection," *IEEE Trans. Power Electron.*, vol. 23, no. 3, pp. 1085–1092, May 2008.

[3] M. Popat, B. Wu, and N. R. Zargari, "A novel decoupled interconnecting method for current-source converter-based offshore wind farms," *IEEE Trans. Power Electron.*, vol. 27, no. 10, pp. 4224–4233, Oct. 2012.

[4] M. E. Baran, H. Hooshyar, Z. Shen, and A. Huang, "Accommodating high PV penetration on distribution feeders," *IEEE Trans. Smart Grid*, vol. 3, no. 2, pp. 1039–1046, Jun. 2012.

[5] A. Yazdani and P. P. Dash, "A control methodology and characterization of dynamics for a photovoltaic (PV) system interfaced with a distribution network," *IEEE Trans. Power Del.*, vol. 24, no. 3, pp. 1538–1551, Jul. 2009.

[6]Christo Ananth, [Account ID: AORZMT9EL3DL0],"A Detailed Analysis Of Two Port RF Networks - Circuit Representation [RF & Microwave Engineering Book 1]", Kindle Edition, USA, ASIN: B06XQY4MVL, ISBN: 978-15-208-752-1-7, Volume 8, March 2017, pp:1-38.

[7] Y. Li, L. Luo, C. Rehtanz, S. Rüberg, and D. Yang, "An industrial DC power supply system based

ISSN 2394-3777 (Print)
ISSN 2394-3785 (Online)
Available online at www.ijartet.com
International Journal of Advanced Research Trends in Engineering and Technology
Vol. 4, Special Issue 2, January 2017

on an inductive filtering method," *IEEE Trans. Ind. Electron.*, vol. 59, no. 2, pp. 714–722, Feb. 2012.

[8] A. R. Oliva and J. C. Balda, "A PV dispersed generator: A power quality analysis within the IEEE 519," *IEEE Trans. Power Del.*, vol. 18, no. 2, pp. 525–530, Apr. 2003.

[9] M. Aiello, A. Cataliotti, S. Favuzza, and G. Graditi, "Theoretical and experimental comparison of total harmonic distortion factors for the evaluation of harmonic and interharmonic pollution of grid-connected photovoltaic systems," *IEEE Trans. Power Del.*, vol. 21, no. 3, pp. 1390–1397, Jul. 2006.

[10] S. H. E. A. Aleem, A. F. Zobaa, and M. M. A. Aziz, "Optimal –type passive filter based on minimization of the voltage harmonic distortion for nonlinear loads," *IEEE Trans. Ind. Electron.*, vol. 59, no. 1, pp. 281–289, Jan. 2012.

[11] H. Akagi and K. Isozaki, "A hybrid active filter for a three-phase 12-pulse diode rectifier used as the front end of a medium-voltage motor drive," *IEEE Trans. Power Electron.*, vol. 27, no. 1, pp. 69–77, Jan. 2012.

[12] C.-S. Lam, W.-H. Choi, M.-C. Wong, and Y.-D. Han, "Adaptive dc-link voltage-controlled hybrid active power filters for reactive power compensation," *IEEE Trans. Power Electron.*, vol. 27, no. 4, pp. 1758–1772, Apr. 2012.

[13] G. Bhuvaneswari and B. C. Mahanta, "Analysis of converter transformer failure in hvdc systems and possible solutions," *IEEE Trans. Power Del.*, vol. 24, no. 2, pp. 814–821, Apr. 2009.

[14] J. A. C. Forrest and B. Allard, "Thermal problems caused by harmonic frequency leakage fluxes in three-phase, three-winding converter transformers," *IEEE Trans. Power Del.*, vol. 19, no. 1, pp. 208–213, Jan. 2004.

[15] M. J. Heathcote, *J&P Transformer Book*, 12th ed. Oxford, U.K.: Reed Educational and Professional Publishing Ltd., 1998.

[16] J. Biela, D. Hassler, J. Schönberger, and J. W. Kolar, "Closed-loop sinusoidal input-current shaping of 12-pulse autotransformer rectifier unit with impressed output voltage," *IEEE Trans. Power Electron.*, vol. 26, no. 1, pp. 249–259, Jan. 2011.

[17] Y. Li, L. Luo, C. Rehtanz, D. Yang, S. Rüberg, and F. Liu, "Harmonic transfer characteristics of a new HVDC system based on an inductive filtering method," *IEEE Trans. Power Electron.*, vol. 5, no. 5, pp. 2273–2283, May 2012.

[18] Y. Li, L. Luo, C. Rehtanz, S. Rüberg, and F. Liu, "Realization of reactive power compensation near the LCC-HVDC converter bridges by means of an inductive filtering method," *IEEE Trans. Power Electron.*, vol. 27, no. 9, pp. 3908–3923, Sep. 2012.

[19] Y. Li, Z. Zhang, C. Rehtanz, L. Luo, S. Rüberg, and F. Liu, "Study on steady- and transient-state characteristics of a new HVDC transmission system based on an inductive filtering method," *IEEE Trans. Power Electron.*, vol. 26, no. 7, pp. 1976–1986, Jul. 2011.

[20] Y. Li, L. Luo, C. Rehtanz, K. Nakamura, J. Xu, and F. Liu, "Study on characteristic parameters of a new converter transformer for HVDC systems," *IEEE Trans. Power Del.*, vol. 24, no. 4, pp. 2125 2131, Oct. 2009.

[21] Y. Li, L. Luo, C. Rehtanz, C. Wang, and S. Rüberg, "Simulation of the electromagnetic response characteristic of an inductively filtered HVDC converter transformer using field-circuit coupling," *IEEE Trans. Ind. Electron.*, vol. 59, no. 11, pp. 4020–4031, Nov. 2012.

[22] H. Akagi, Y. Kanazawa, and A. Nabae, "Instantaneous reactive power compensators comprising switching devices without energy storage components," *IEEE Trans. Ind. Appl.*, vol. IA-20, no. 3, pp. 625–630, May 1984.

[23] *"PSCAD/EMTDC Manuals,"* Manitoba HVDC Research Center, Winnipeg, MB, Canada.